Since January 2020 Elsevier has created a COVID-19 resource centre with free information in English and Mandarin on the novel coronavirus COVID-19. The COVID-19 resource centre is hosted on Elsevier Connect, the company's public news and information website.

Computers in Biology and Medicine 146 (2022) 105625

Contents lists available at ScienceDirect

Computers in Biology and Medicine

journal homepage: www.elsevier.com/locate/compbiomed

Inhibition of SARS-CoV-2 pathogenesis by potent peptides designed by the mutation of ACE2 binding region

Saeed Pourmand [a,1], Sara Zareei [b,c,1], Mohsen Shahlaei [e,*], Sajad Moradi [e,**]

[a] Department of Chemical Engineering, Faculty of Chemical and Petroleum Engineering, University of Tabriz, Tabriz, Iran
[b] Department of Cell & Molecular Biology, Faculty of Biological Sciences, Kharazmi University, Tehran, Iran
[c] Department of Medicinal Chemistry, Faculty of Pharmacy, Tehran University of Medical Sciences, Tehran, Iran
[e] Nano Drug Delivery Research Center, Health Technology Institute, Kermanshah University of Medical Sciences, Kermanshah, Iran

ARTICLE INFO

Keywords:
COVID-19
Peptide design
SARS-CoV-2
Antiviral peptide
Viral entry inhibitors

ABSTRACT

The outbreak of COVID-19 has resulted in millions of deaths. Despite all attempts that have been made to combat the pandemic, the re-emergence of new variants complicated SARS-CoV-2 eradication. The ongoing global spread of COVID-19 demands the incessant development of novel agents in vaccination, diagnosis, and therapeutics. Targeting receptor-binding domain (RBD) of spike protein by which the virus identifies host receptor, angiotensin-converting enzyme (ACE2), is a promising strategy for curbing viral infection. This study aims to discover novel peptide inhibitors against SARS-CoV-2 entry using computational approaches. The RBD binding domain of ACE2 was extracted and docked against the RBD. MMPBSA calculations revealed the binding energies of each residue in the template. The residues with unfavorable binding energies were considered as mutation spots by OSPREY. Binding energies of the residues in RBD-ACE2 interface was determined by molecular docking. Peptide inhibitors were designed by the mutation of RBD residues in the virus-receptors complex which had unfavorable energies. Peptide tendency for RBD binding, safety, and allergenicity were the criteria based on which the final hits were screened among the initial library. Molecular dynamics simulations also provided information on the mechanisms of inhibitory action in peptides. The results were finally validated by molecular docking simulations to make sure the peptides are capable of hindering virus-host interaction. Our results introduce three peptides P7 (RAWTFLDKFNHEAEDLRYQSSLASWN), P13 (RASTFLDKFNHEAEDLRYQSSLASWN), and P19 (RADTFLDKFNHEAEDLRYQSSLASWN) as potential effective inhibitors of SARS-CoV-2 entry which could be considered in drug development for COVID-19 treatment.

1. Introduction

Peptides with therapeutic potential have been considered during the last decades and the number of FDA-approved peptide drugs has increased [1]. They offer several advantages like ease of synthesis, high specificity, and limited accumulative behavior. These benefits have made peptides favorable agents in the development of diagnostic approaches, vaccines, and drugs against highly infectious viruses including influenza, acquired immunodeficiency syndrome, chronic hepatitis B, dengue virus, and coronavirus disease 2019 [2,3]. Moreover, antiviral peptides (AVPs) have the potential to block a virus' cycle at different levels from viral attachment to the host cell to its replication. Some AVPs have natural origins [4–7] while others are discovered or rationally designed by bioinformatics techniques machine learning [8–11]. Since the outbreak of COVID-19, which is caused by the SARS-CoV-2 virus, peptide inhibitors have also been among the promising anti-covid agents from various resources [12]. While some studies seek to find peptide anti-COVID-19 agents from natural resources [13], others tried to rationally design novel peptides [12].

Due to the importance of the entrance step in the pathogenesis of viruses as obligate intracellular parasites, it has been the main target for anti-viral development. This is also the case about SARS-CoV-2 whose pathogenesis depends on angiotensin-converting enzyme II as a receptor [14–16] to either directly fuse its genetic materials into the cell or enter

* Corresponding author.
** Corresponding author.
E-mail addresses: mohsenshahlaei@yahoo.com, sajad.moradi@kums.ac.ir (M. Shahlaei), sajadmoradi28@gmail.com, mshahlaei@kums.ac.ir (S. Moradi).
[1] Equal contribution.

https://doi.org/10.1016/j.compbiomed.2022.105625
Received 27 December 2021; Received in revised form 10 March 2022; Accepted 4 April 2022
Available online 17 May 2022

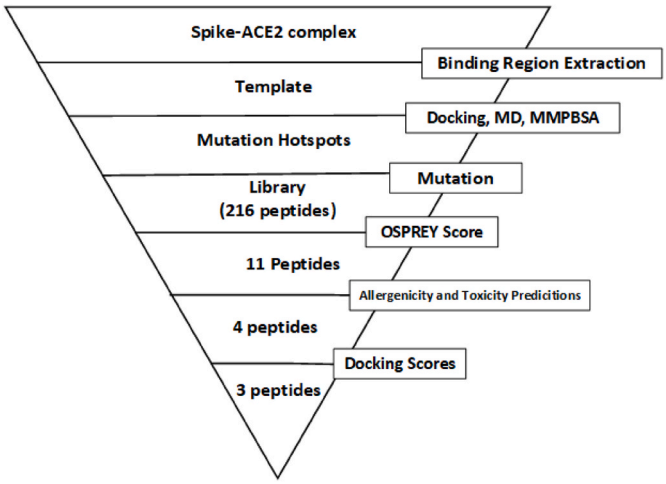

Fig. 1. The research overall design and flow process.

in endosome-based endocytosis [17]. Host receptor recognition is mediated by the SARS-CoV-2 spike S1 subunit which is expressed on the viral envelope. Four main domains make up S, one of which is located in the direct interaction with ACE2, named receptor-binding domain (RBD) [15,18]. On the receptor side, the N-terminal helix of ACE2 is recognized by RBD and interacts with the virus [16,19].

Peptide inhibitors against SARS-CoV-2 entry have been proposed using three main strategies. Firstly, many peptides focused on virus fusion. This process is made possible by the catalytic cleavage of spike protein by the host proteases TMPRSS2 (transmembrane protease serine 2), furin, and cathepsin-L [20–22], is shown that can be blocked by peptides [23–27]. The second strategy is approached by receptor antagonists. The peptides in this category are designed or shown to block virus entry by occupying the host N-terminal helix of ACE2 [28,29]. While fusion inhibitors and receptor antagonists must approach the host cell to perform their anti-COVID-19 activity, in the last category, virus inactivators, peptides can prevent the viral infection before the virus achieve ACE2 N-helix in blood. These inhibitors mostly interact with the SARS-CoV-2 RBD domain and neutralize its binding affinity for ACE2 [30–32].

As the computational methods provide the cost and time effective manner for investigating the biomolecular interactions in detailed state [33,34], in this study, we applied computational approaches with the mutation-based rational design of peptides to prevent host cell recognition mediated by the SARS-CoV-2 RBD domain, thereby discovering peptides with potential competitive affinity for blocking viral pathogenesis.

2. Materials and methods

The overall diagram of the methods is illustrated in Fig. 1.

2.1. Interface analysis and template extraction

ACE2 residues that embrace viral spike RBD were considered as an inspiration for inhibitor design due to their ability to form a stable complex with the virus. Therefore, the peptides which can mimic the binding behavior of the virus binding region may interfere with the viral attachments and subsequently, may prevent viral fusion and pathogenesis.

The PDB structure of SARS-CoV2 RBD complexed with ACE2 (PDB ID: 6m0j) was obtained from the RCSB protein data bank (https://www.rcsb.org/) and the interactions in the interface of the virus and the receptor were identified and visualized by LigPlot^{+} v. 2.2.4 [35].

2.2. Molecular docking and molecular dynamics simulations

Molecular dockings were carried out applying the fully-automated ClusPro server (https://cluspro.org/) [36,37] to estimate spike-peptides binding modes. This server needs a simple provision of two molecule files being introduced as a receptor or peptide. ClusPro considers both molecules as rigid and automatically docks them using a fixed grid box for the receptor and a movable grid for the peptide. The docking score is calculated based on the following equation in ClusPro:

$$E = w_1E_{rep} + w_2E_{attr} + w_3E_{elec} + w_4E_{DARS}$$

Here, E_{rep}, E_{attr}, and E_{elect} represent the repulsive and attractive contribution to the van der Waals interaction and electrostatic energy, respectively. E_{DARS} denotes the Decoys as Reference State (DARS) approach which is measured by the amount of free energy change following the removal of water molecules from the protein interface. This parameter takes the desolvation contribution into account. W1-4 coefficients are weighted which is calculated for different types of docking problems [36].

After the separate introduction of the receptor's and peptides' files to the server, each run was performed for the receptor and a peptide with default parameters. Among the results, the conformations with the lowest docking scores were selected for further analysis.

In molecular dynamics (MD) simulations, the candidate peptides-ACE2 complexes were put into a 100-ns simulation using GROMACS package v. 2020 [38], Gromos96 54a7 [39], and SPCE water model. Gromos 96 was selected since it has a favorable agreement with the NMR data and the X-ray crystal structure of the protein [40]. Each complex was centered in a cubic box with a minimum distance of 1.0 nm from the edges. The energy of all systems was minimized for 50,000 steps followed by a thermal equilibrium step using Berendsen thermostat at 310 K. The pressure was equilibrated for 1 ns to achieve the pressure of 1 bar using Berendsen barostat, LINCS algorithm [41] for bond constrain, and PME mesh [42] for the calculation of long-range electrostatic interactions. Moreover, the Fourier grid spacing and Coulomb radius were set at 0.16 and 1.2 nm, respectively, and the van der Waals interactions were limited to 1.2 nm. Finally, the production states were performed under the leapfrog algorithm for 100 ns?

The resulted trajectories were then analyzed by built-in GROMACS utilities e.g. root mean squared deviation (RMSD), root mean squared fluctuation (RMSF), radios of gyration(Rg), principle component analysis (PCA) and solvent accessible surface area (SASA).

2.3. Binding energy calculation

To identify how important is the contribution of each reside in spike binding, the resides of decoy peptide was analyzed using g_mmpbsa program [43], the definitions of which can be applied to our system as

$$\Delta G_{Binding} = \Delta G_{Spike-template} - (\Delta G_{Spike} + \Delta G_{Template})$$

Where $\Delta G_{Spike-template}$, ΔG_{Spike}, and $\Delta G_{Template}$ describe the total energy of spike-template peptide complex, solution free energy of spike, and solution free energy of free template peptide, respectively.

2.4. Library construction

Peptide library was built by OSPREY v. 3.0 (Open-Source Protein Redesign for You) [44] python-based script in which the input pdb files of the template was introduced as a strand. The mutation hotspots were then defined by strand. Flexibility and the probable residues of Ile, Trp, Ser, Thr, and Asp were determined by setLibraryRotamers scripts, respectively. The defined strand was used to make a conf space and the osprey forcefield parameters were selected. The remained scripts were performed as with default parameters according to the OSPREY documentation.

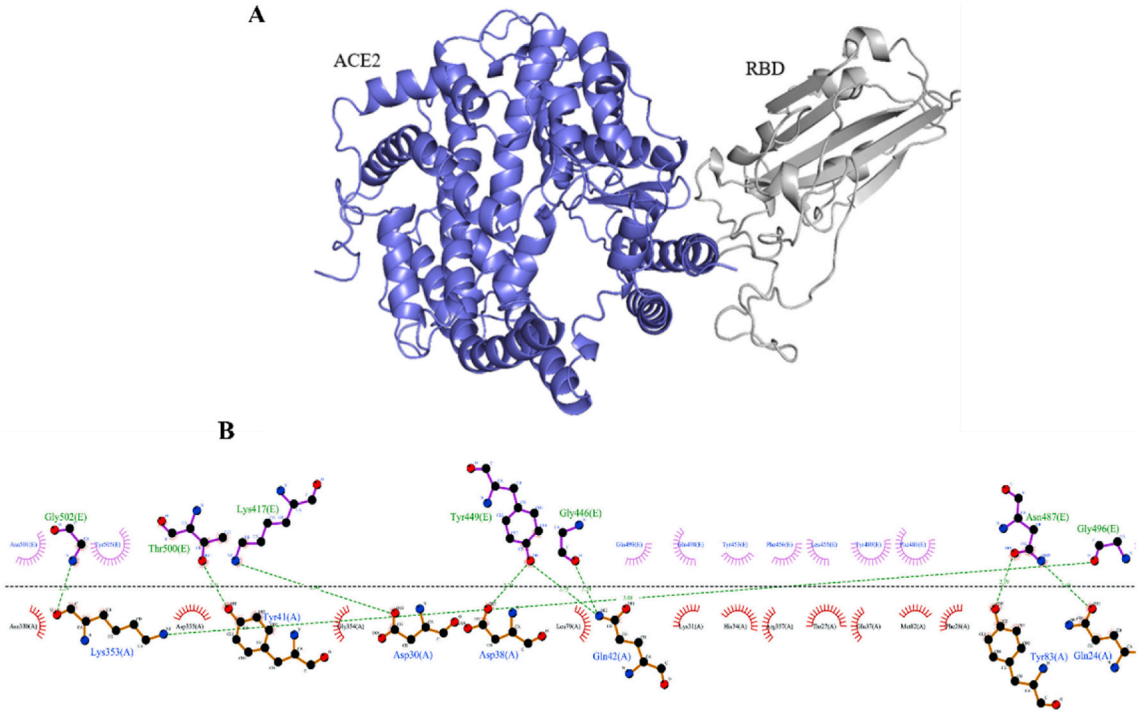

Fig. 2. The illustration of (A) ACE2-RBD complex and (B) the interactions made by ACE2 and SARS-Cov-2 RBD. The viral residues with hydrogen bonds and hydrophobic forces are indicated by pink and blue fonts and the green and black fonts indicate ACE2 residues with hydrophobic and hydrogen bonds, respectively. The atoms with H-bonds are connected with green dashed lines.

Table 1
The mmpbsa energy analysis of the template residues revealed by a 100-ns MD simulation.

Template Residue	$\Delta G_{binding}$ (kJ/mol)
24GLN	64.533
25ALA	−5.905
26LYS	77.717
27THR	−20.011
28PHE	−21.064
29LEU	−5.489
30ASP	−74.37
31LYS	52.018
32PHE	−3.903
33ASN	−8.814
34HIS	−0.822
35GLU	−80.445
36ALA	−0.604
37GLU	−116.525
38ASP	−107.831
39LEU	−5.742
40PHE	0.095
41TYR	−13.531
42GLN	−3.413
43SER	−5.584
44SER	−4.1
45LEU	−16.746
46ALA	−7.268
47SER	−6.086
48TRP	−14.855
49ASN	−111.155

2.5. Validation of toxicity and allergenicity

The toxicity and allergenicity properties of screened peptides were predicted by ToxinPred (https://webs.iiitd.edu.in/raghava/toxinpred/protein.php) [45] and AllerTop v. 2.0 (http://www.ddg-pharmfac.net/AllerTOP/) servers [46]. Both servers offer fully automated predictions which need peptide sequence as input. In ToxinPred, fragment length of 10 residues and other default parameters were set.

Table 2
The inhibitory peptides with the highest OSPREY scores and the assessment of their allergenicity.

ID	Peptide Inhibitor	OSPERY Score	Allergenicity
1	RARTFLDKFNHEAEDLRYQSSLASWN	−90.6	PROBABLE ALLERGEN
109	DARTFLDKFNHEAEDLRYQSSLASWN	−79.6	PROBABLE ALLERGEN
19	**RADTFLDKFNHEAEDLRYQSSLASWN**	**−77.7**	**Non**
37	WARTFLDKFNHEAEDLRYQSSLASWN	−74.7	PROBABLE ALLERGEN
4	RARTFLDKFNHEAEDLDYQSSLASWN	−73.4	PROBABLE ALLERGEN
181	TARTFLDKFNHEAEDLRYQSSLASWN	−72.6	Non
7	**RAWTFLDKFNHEAEDLRYQSSLASWN**	**−72.6**	**Non**
73	SARTFLDKFNHEAEDLRYQSSLASWN	−72.4	PROBABLE ALLERGEN
31	RATTFLDKFNHEAEDLRYQSSLASWN	−71.9	PROBABLE ALLERGEN
13	**RASTFLDKFNHEAEDLRYQSSLASWN**	**−71.8**	**Non**
2	RARTFLDKFNHEAEDLWYQSSLASWN	−71.7	PROBABLE ALLERGEN

3. Results and discussion

It is well known that the SARS-COV-2 virus is equipped with a glycoprotein anchor, Spike (S), which guarantees host cell recognition and viral entry by interacting with angiotensin-converting enzyme 2 (ACE2) which is expressed on the surface of human cells [1,2]. Spike protein has been the initial main target for drug design. It is formed by S1 and S2 subunits, both of which are comprised of various domains. While the S1 subunit is known to be responsible for cell recognition, the S2 subunit plays a vital role in membrane fusion, following which the viral entry occurs. However, it is following the direct establishment of

Table 3
The comparison of sequence, binding affinities (docking scores), and interactions of the template and top hits of computationally improved peptides binding. The residues involved in H-binding are indicated in bold.

ID	Sequence	Clus Pro Docking Score	Residues	
			Spike RBD	Peptide
Template	QAKTFLDKFNHEAEDLFYQSSLASWN	−700.6	**Lys417**, **Gly446**, **Tyr449**, Tyr453, Leu455, Phe456, Ala475, **Asn487**, Tyr489, Gln493, Gln498, **Thr500**, Asn501, Tyr505	**Gln24**, Thr27, phe28, **Asp30**, Lys31, His34, Glu37, **Asp38**, **Tyr41**, **Gln42**
P7	RAWTFLDKFNHEAEDLRYQSSLASWN	−761.6	**Arg403**, **Lys417**, Gly446, Gly447, **Tyr449**, **Tyr453**, Leu455, Tyr473, **Tyr489**, **Gln493**, Gln498, **Tyr500**, **Asn501, Tyr505**	Ala25, **Trp26**, Phe28, Leu29, **Asp30**, Lys31, **His34, Glu37, Asp39**, Tyr41, Gln42
P13	RASTFLDKFNHEAEDLRYQSSLASWN	−726.6	**Tyr453**, Leu455, Phe456, Tye473, Tyr489, **Gln493**, Tyr495, **Gly496**, Phe497	Thr27, Phe28, **Lys31**, **Asp38**, **His34**, Gln42
P19	RADTFLDKFNHEAEDLRYQSSLASWN	−730.1	**Lys417**, Gly446, Gly447, Asn448, **Tyr449**, **Asn450**, Tyr451, Tyr453, Leu455, **Phe456**, Arg457, Tyr473, Ala475, **Tyr489**, **Leu492**, **Gln493**, **Gln498**	**Thr27**, Phe28, **Asp30**, **Lys31**, His34, Glu35
P181	TARTFLDKFNHEAEDLRYQSSLASWN	−673.1	**Lys417**, Lys444, Val445, **Gly447**, Asn448, **Tyr449**, **Tyr453**, Leu455, Phe456, Tyr489, Gln493, **Ser494**, Gly496, **Gln498**, Tyr505	Thr27, **Asp30**, Lys31, **His34**, Glu37, **Tyr41**, Gln42, Leu45, **Trp48**

interaction between the S1 and ACE2 peptidase domain that the spike undergoes proteolytic cleavage, and the viral infection initiates [47]. S1 includes a domain called receptor-binding domain (RBD) (residues 333–526) with two main subdomains: five anti-parallel β-sheets (e.g., β1, β2, β3, β4, and β7) and connecting loops. α4, β5, β6, and α5 form a region named receptor-binding motif (RBM) and it includes most of the residues responsible for receptor binding [16,19]. A variety of inhibitors have been proposed for hindering ACE2-RBD interaction small inhibitors [48], antibodies [49], phytochemicals [50], and FDA-approved drugs [51,52].

Whether the SARS-CoV-2's genetic material enters the cytoplasm directly or the whole virus makes use of endosomes for cell penetration, both mechanisms require ACE2 recognition by its RBD domain. Therefore, RBD binders may inhibit viral attachment to the receptor and subsequently perform as a virus inactivator. In the present study, ACE2-derived peptides were computationally designed based on the RBD-binding residues of ACE2 and their potential propensities were predicted using computer-aided approaches.

To construct a peptide inhibitor library, the interactions that bind SARS-CoV-2 to the host ACE2 were praised using the experimentally approved PDB structure of their complex. Among the residues shown in Fig. 2, ACE2 residues which are targeted by the virus were Gln24, Thr27, Phe28, Asp30, Lys31, His34, Glu37, Asp38, Tyr41, Gln42, Leu79, Met82, Tyr83, Asn330, Lys353, Gly354, Asp355, and Arg357.

We chose the ACE2 chain A residues placed in 24–49 positions as a template peptide for inhibitor design. The selection of this region is supported by alanine scanning results that showed the critical role of residues 22–57 for S1 attachment [53]. The template was then docked against spike protein to validate its binding potential. The docking result showed that it chose the RBM motif for binding, as the source PDB, with the binding score of −700.6. The designed peptide, therefore, must have greater negative energy than the template and a higher affinity for RBD than the receptor to effectively prohibit the virus-receptor interaction.

The template-receptor complex was put into 100ns of MD simulation to reveal the spots where their interactions are relatively weak and can be substituted by other amino acids in sequence. MMPBSA calculation indicated that the residues 24, 26, 31, and 40 had unfavorable binding energies suggesting their negative effect on binding the spike to ACE2 (Table 1). This offers an opportunity to design peptide inhibitors with stringer binding affinity.

Following the mutation-based peptide design, a peptide library of 216 unique sequences was constructed using OSPREY (Table S1). Several studies introduced peptide inhibitors against RBD. However, they used different approaches to design peptides [54–60], and therefore, their results may seem incomparable to the present study. In the next step, 11 peptides having the greatest OSPREY scores were chosen and their probable allergenicity and toxicity were evaluated. As shown in Table 2, peptides **19**, **181**, **7**, and **13** were allergically safe. Having no toxicity, these four peptides were considered as final candidates for docking simulations using the Clus pro server.

The results showed that except for peptide **P181** (−673.1), other designed peptides had greater binding scores compared to template peptides (−761.6, −726.6, and −730.1 for **P7**, **P13**, and **P19**) (Table 3). This suggests that peptides **P7**, **P13**, and **P19** had a higher affinity for spike protein, with peptide **P7** having the highest affinity.

The higher binding potential of **P7** may be explained by its highest number of hydrogen bonds (five) and the highest number of spike residues involved in its binding (Table 3). Among the viral residues, Arg403 was only connected with **P7** while others formed interactions with at least two peptides (Fig. 3). Moreover, it is evident from Fig. 3 that three peptides attached the RBM motif so that α4, β5, β6, and α5 are involved. It has been established by previous studies that the RBD position which virus apply in receptor recognition lie in two regions: 1) locations 190, 493–495, 498, 501 and 502 and 2) 417 and 458. Since the selected peptides were able to block both regions, this can be a clear evidence for their potential to directly inhibit spike-ACE2 interaction and viral entering to the host cells [16,61] (Fig. 3).

RMSD analysis was applied to study the equilibration and stability of each system. As can be seen in Fig. 4, the higher values of *RMSD* were observed for **P7** and **P19** complexes indicating higher instability in protein dynamics as a result of peptide binding. In contrast, the value of *RMSD* for **P13**-RBD was in line with that of template peptide. This suggests that the conformational changes in RBD induced by **P7** and **P19** were more severe than those of other system (Fig. 4).

Rg analysis which is an indicator of protein compactness is interpreted as a characteristic of protein stability [62]. The results showed that the interaction of all peptides with RBD caused a little compactness in protein structure. There are also significant fluctuations in the *Rg* diagram of the **P7** complexed RBD which show there is recurrent open/close in protein structure indicating the binding of peptide to protein lead to instability in its structure (Fig. 4B).

Solvent accessible surface area (*SASA*) of proteins is a surface around a protein determined by a hypothetical center of a solvent sphere which has van der Waals contact surface with the protein. The results obtained in *SASA* analysis are shown in Fig. 4C and as can be seen there is no significant changes in the final values of *SASA* in all studied systems (Fig. 4C). This is a sign for the systems that did not undergo high values of opening or compactness which is in agreement with the results of *Rg*.

RMSF analysis also gained information about the volatility of each RBD residue during the simulation. It is evident from Fig. 4D that the greatest amino acid fluctuation is seen in the RBD when it is complexed with **P7**. This in line with the results obtained from other MD analysis which indicated that this peptide forces the protein to possess higher mobility which can lead to instability in its structure. Definition Secondary Structure of Protein (*DSSP*) gives information about the frequency of each secondary structure in protein's conformation. *DSSP*

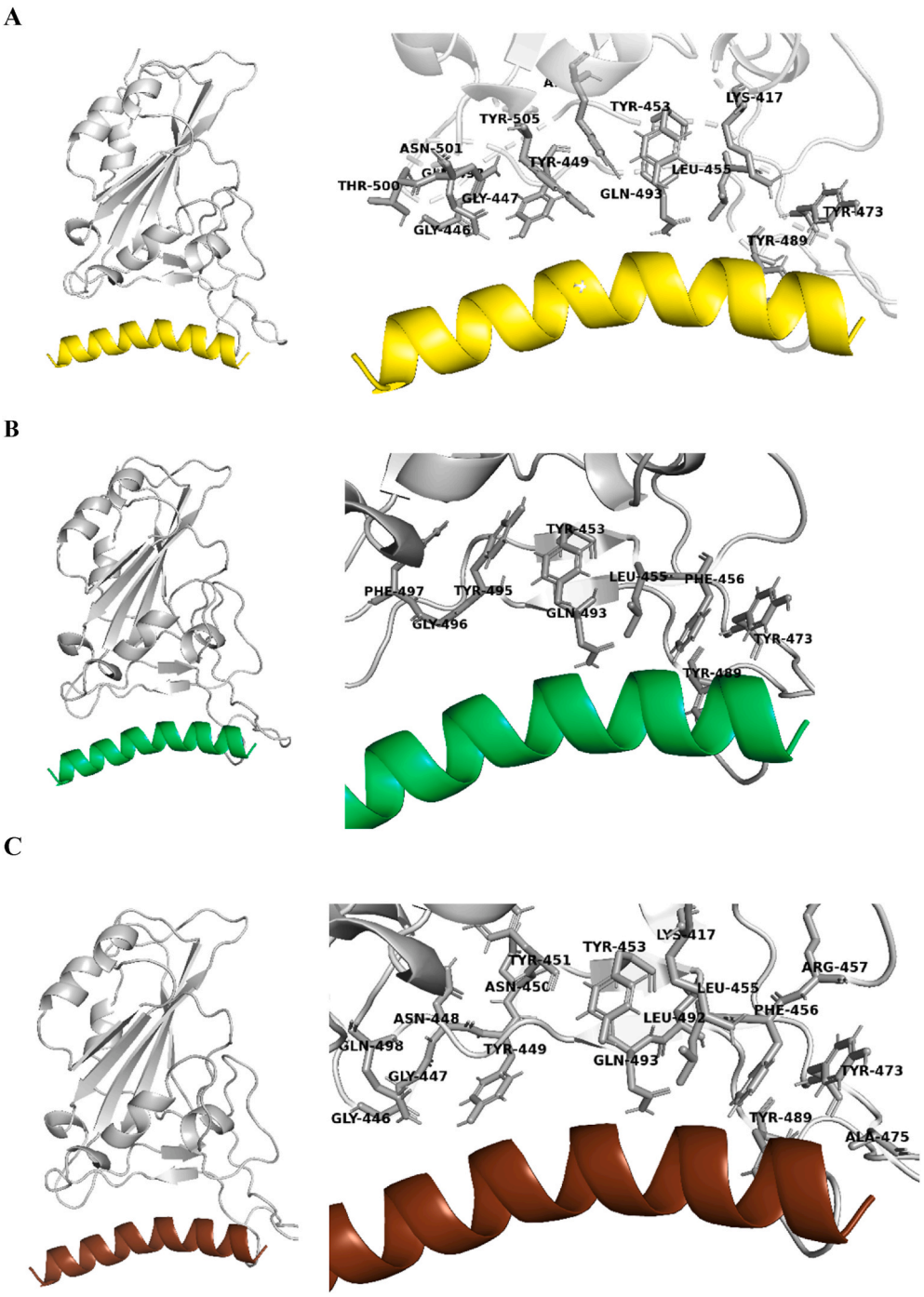

Fig. 3. The representations of the best docking pose of top three peptides (A) P7, B) P13, and C) P19) bound to the RBD (gray) domain of the SARS-CoV-2 with the best docking scores.

analysis also revealed no significant changes in various types of secondary structures over the span of simulation time (Table 4). Principal Component Analysis (*PCA*) provides the main components of protein motion during the simulation [63]. The 2D diagram of the RBD movements for different systems was obtained using the projection of the first two principal components. As can be seen in Fig. 5, the **P7**-RBD pattern in more propagated over the diagram plane indicating the higher protein flexibility and movements in this system which is in good agreement with other results.

The number of hydrogen bonds was also investigated since they are the main interactions that stabilize a complex. The number of H-bonds during 100 ns simulations varied for each peptide. In comparison with other two peptides the results indicated that P7 formed more stable hydrogen bonds with the RBD (Fig. 6).

Furthermore, the free non-bonded binding energies (e.g., van der Waals, electrostatic, polar solvation, and SASA energy) of the final systems were calculated using MM/PBSA method. The binding energies between spike RBD domain and peptides during the whole simulation revealed that **P19** had a stronger interaction with the spike however other binding energies are also potent for complex formation (Table 5). These results are also in good agreement with that of docking results.

Finally the resulted RBD-peptide complexes were docked against host receptor to validate their inhibitory activity. As shown in Fig. 7, the RBD domain proved divergence from the position it must take to infect

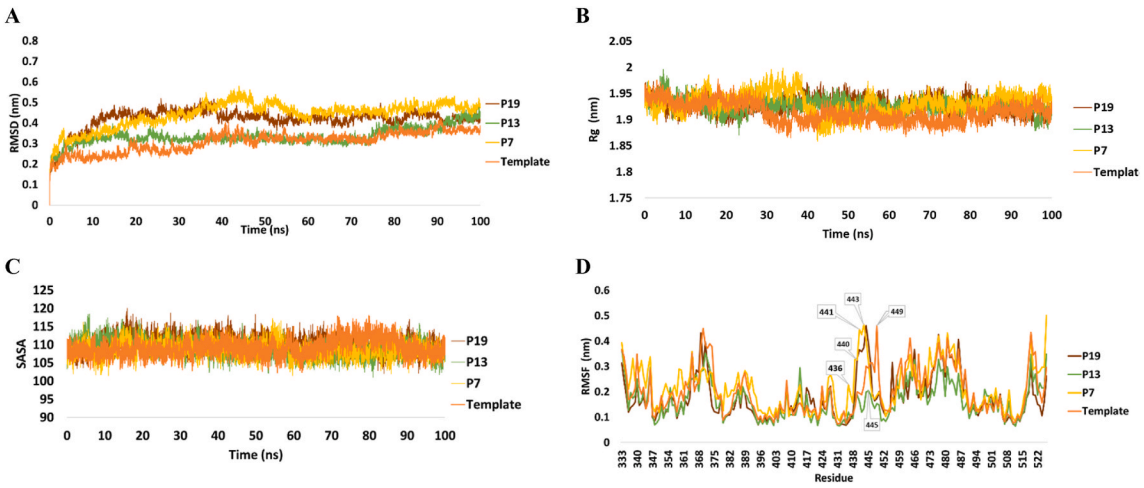

Fig. 4. Trajectory analysis of the final peptide hits compared to the template in terms of RMSD(A), Rg(B), SASA(C), and RMSF (D) in complex with RBD domain of SARS-CoV-2 spike.

Table 4
The frequency of secondary structures in RBD in complex with selected peptides compared with the template.

ID	Structure	Coil	B-Sheet	B-Bridge	Bend	Turn	A-Helix	3-Helix
Template	0.49	0.32	0.28	0.02	0.16	0.11	0.08	0.03
P7	0.49	0.32	0.26	0.03	0.17	0.1	0.1	0.02
P13	0.49	0.33	0.26	0.03	0.16	0.08	0.12	0.02
P19	0.48	0.31	0.26	0.03	0.17	0.11	0.08	0.03

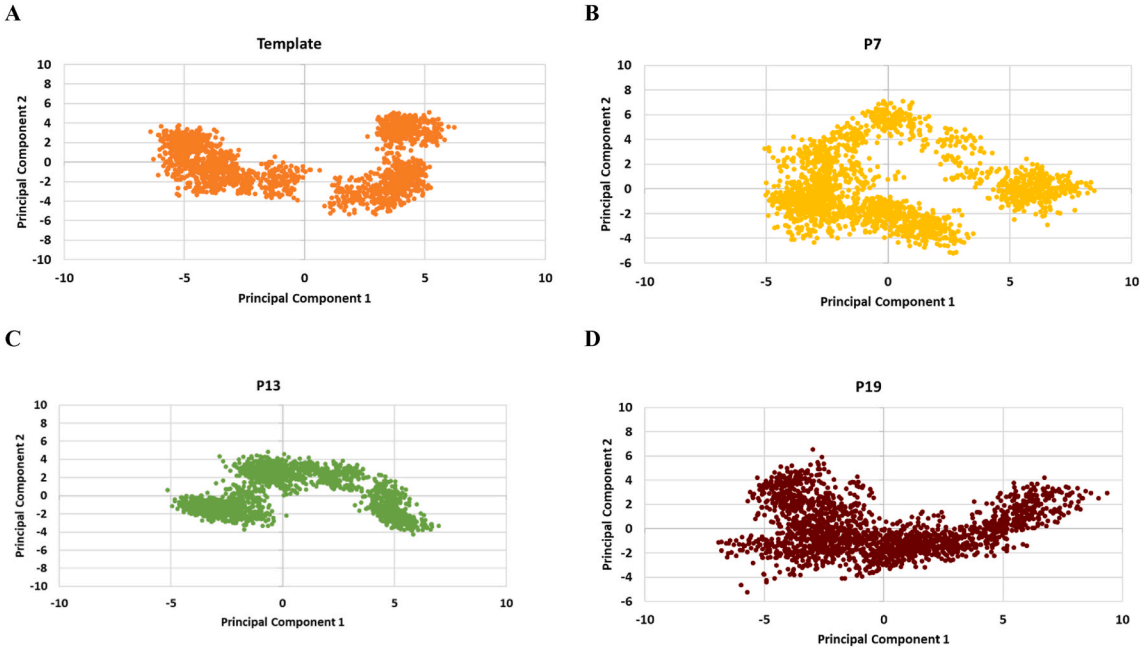

Fig. 5. Trajectory analysis of the final peptide hits compared to the template in terms of RMSD(A), Rg(B), SASA(C), and RMSF (D) in complex with RBD domain of SARS-CoV-2 spike.

the host cell. As it can be seen, binding the peptides **P7** and **P13** to the protein resulted in non-proper binding of the spike RBD with the ACE2. The amino acids involve in RBD-receptor binding are listed in Table 6 for all complexes. In previous studies the vital role of RBD Lys417 is approved in the virus binding affinity, transmission, and immune escape by mutation analysis [64]. Accordingly, **P7** and **P13** might be preferable since they successfully limited this residue. Moreover, the energetic assessment of residues lying in the RBD-ACE2 complex indicated the stabilizing impact of Tyr449, Leu455, Phe456, Ala475, Phe486, Glu493, Gly496, Gln498, Thr500, Asn501, Gly502, and Tyr505 in the virus-host complex formation [65]. Also it can be seen that **P7** let only 3 RBD residues (Phe456, Asn501, and Tyr505) to access the receptor. However, this number increased to 4 and 6 residues for **P13** (Leu455, Phe456, Gln493, and Gly496) and **P19** (Tyr449, Leu455, Phe456, Ala475, Gln493, and Gln498). Regarding ACE2, X-ray diffraction experiments demonstrated residues Gln24, Lys31, Tyr41, Gln42, Leu79, Met82,

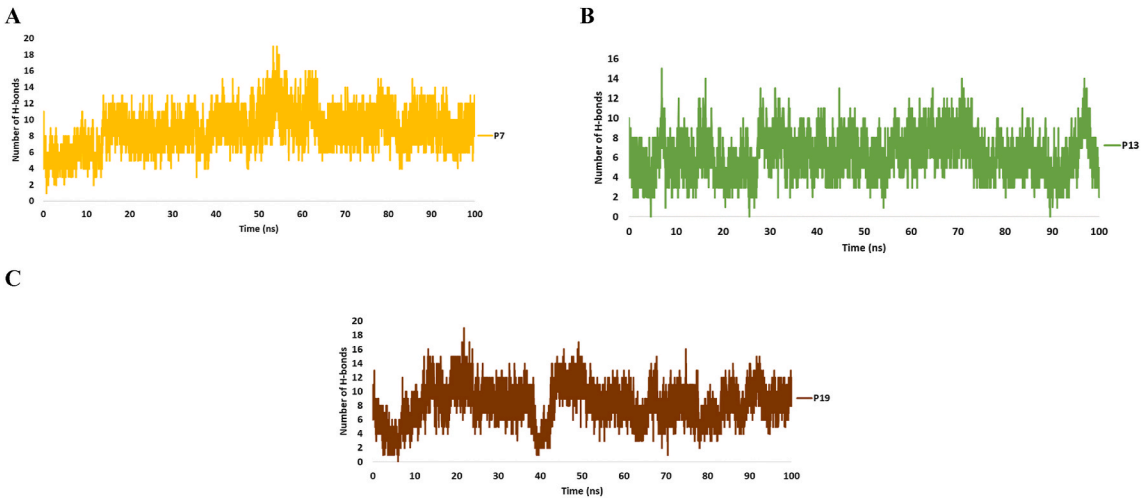

Fig. 6. Estimation of hydrogen bonds of candidate peptides P7 (A), P13 (B), and P19(C) with RBD domain of SARS-CoV-2 spike over the span of 100 ns?

Table 5
Energy profiles of RBD domain of spike in complex with the template, P7, P13, and P19.

ID	Van der Waal Energy (kJ/mol)	Electrostatic Energy (kJ/mol)	Polar Solvation Energy (kJ/mol)	SASA Energy (kJ/mol)	Binding Energy (kJ/mol)
Template	−263.9	−782.2	795.9	−35.9	−286.2
P7	−244.9	−631.2	660.6	−32.7	−248.2
P13	−222.6	−479.9	563.2	−29.6	−169.0
P19	−252.6	−739.7	726.0	−34.8	−301.2

Tyr83, and Lys353 as essential elements for viral recognition [16]. In control docking, it is evident that ACE2 could involve its vital residues the most when bound to **P7** with Lys31, Tyr41, Gln42, Tyr83, and Lys353 but fewer host residues were involved due to the inhibition of **P13** (ACE2 Lys31, and Gln42) and **P19** (ACE2 Lys 31). These data suggest that although **P19** and **P13** let several important pathogenic RBD residues free, they hindered RBD to accommodate the ACE2 recognition region. In contrast, **P7** stifled the RBD-ACE2 complex formation by preventing most of RBD determinant residues.

4. Conclusion

In the present study, a library of 216 peptides was designed to investigate their inhibitory potential in complex formation of RBD domain of SARS-Cov-2 and its main receptor the ACE2. At first using the pre docking and MD simulation analysis the interaction of ACE2 derived peptide and the RBD was evaluated. Among all the obtained peptides, based on the binding scores and biological factors such as immunogenicity and stability, number of 3 peptides was selected for the rest of calculations. the results of molecular dynamic simulation indicated that the P3 peptide causes more instability in protein dynamic. This is extracted from the higher values of *RMSD* and residue *RMSF* during the simulation. Also the more sever fluctuation in the Rg and more distribution in 2D PCA diagrams of the RBD confirmed the noted conclusion. Also the results illustrated that in all systems the h-bonding interactions are a part of complex stabilization forces between the RBD and designed peptide. The results of non-bonded interactions showed that the **P19** peptide performed the more strong interaction with the RBD however others also possess a tight binding to the protein. Finally the docking results confirmed that among the three studied peptides both the **P7** and **P13** have more adverse effects on binding of the RBD to

Table 6
The comparison of interactions between ACE2 host receptor and spike RBD domain when the final designed peptides interfere with their contact. The residues involved in H-binding are indicated in bold.

ID	Residues	
	Spike RBD	ACE2
P7	**Glu406**, **Arg408**, Asp420, Phe456, **Tyr473**, Gly476, Ser477, Asn501, Val503, Tyr505	Thr27, **Lys31**, Tyr41, Gln42, Lys68, **Glu75**, Tyr83, Gly326, Asn330, Lys353, Asp355
P13	**Tyr453**, Leu455, Phe456, Tyr473, Tyr489, **Gln493**, Tyr495, **Gly496**, Phe497	Thr27, Phe28, **Lys31**, **His34**, **Asp38**, Gln42
P19	**Lys417**, Gly446, Gly447, Asn448, **Tyr449**, **Asn450**, Tyr451, Tyr453, Leu455, **Phe456**, Arg457, Tyr473, Ala475, **Tyr489**, **Leu492**, **Gln493**, **Gln498**	**Thr27**, Phe28, **Asp30**, **Lys31**, His34, Glu35

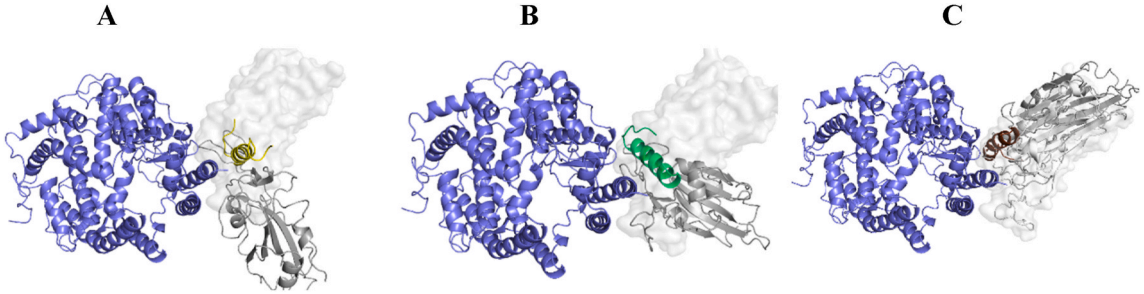

Fig. 7. The representations of the best docking pose of top three peptides (A) P7, B) P13, and C) P19) bound to the RBD (gray) domain of the SARS-CoV-2 with the best docking scores. The surface regions indicate RBD position in receptor recognition.

its receptor. From all the results obtained in this study it can be concluded that the as designed **P7** peptide is capable of being promising blocker of SARS-CoV-2 host cell recognition with high affinity.

Acknowledgment

The authors have acknowledged the Kermanshah University of Medical Sciences for financial supports. Grant number [4000118].

Appendix A. Supplementary data

Supplementary data to this article can be found online at https://doi.org/10.1016/j.compbiomed.2022.105625.

References

[1] L.M. Jarvis, THE NEW DRUGS of 2019 the 48 medicines represent another highly productive year for the pharmaceutical industry, with cancer and rare-disease drugs again dominating the list, Chem. Eng. News 98 (3) (2020) 30–36.
[2] S. Al-Azzam, et al., Peptides to combat viral infectious diseases, Peptides (2020) 170402.
[3] M.-F. Chew, K.-S. Poh, C.-L. Poh, Peptides as therapeutic agents for dengue virus, Int. J. Med. Sci. 14 (13) (2017) 1342.
[4] A. Ahmed, et al., Human antimicrobial peptides as therapeutics for viral infections, Viruses 11 (8) (2019) 704.
[5] L.-j. Zhang, R.L. Gallo, Antimicrobial peptides, Curr. Biol. 26 (1) (2016) R14–R19.
[6] L.C.P. Vilas Boas, et al., Antiviral peptides as promising therapeutic drugs, Cell. Mol. Life Sci. 76 (18) (2019) 3525–3542.
[7] Y. Chand, S. Singh, Prioritization of potential vaccine candidates and designing a multiepitope-based subunit vaccine against multidrug-resistant Salmonella Typhi str. CT18: a subtractive proteomics and immunoinformatics approach, Microb. Pathog. 159 (2021) 105150.
[8] Y. Pang, et al., AVPIden: a new scheme for identification and functional prediction of antiviral peptides based on machine learning approaches, Briefings Bioinf. 22 (6) (2021) bbab263.
[9] N. Thakur, A. Qureshi, M. Kumar, AVPpred: collection and prediction of highly effective antiviral peptides, Nucleic Acids Res. 40 (W1) (2012) W199–W204.
[10] K.Y. Chang, J.-R. Yang, Analysis and prediction of highly effective antiviral peptides based on random forests, PLoS One 8 (8) (2013) e70166.
[11] J. Li, et al., DeepAVP: a dual-channel deep neural network for identifying variable-length antiviral peptides, IEEE Journal of Biomedical and Health Informatics 24 (10) (2020) 3012–3019.
[12] D. Schütz, et al., Peptide and Peptide-Based Inhibitors of SARS-CoV-2 Entry, Advanced Drug Delivery Reviews, 2020.
[13] D. Gentile, et al., Putative inhibitors of SARS-CoV-2 main protease from a library of marine natural products: a virtual screening and molecular modeling study, Mar. Drugs 18 (4) (2020) 225.
[14] Q. Wang, et al., Structural and functional basis of SARS-CoV-2 entry by using human ACE2, Cell 181 (4) (2020) 894–904, e9.
[15] A.C. Walls, et al., Structure, function, and antigenicity of the SARS-CoV-2 spike glycoprotein, Cell 181 (2) (2020) 281–292, e6.
[16] J. Lan, et al., Structure of the SARS-CoV-2 spike receptor-binding domain bound to the ACE2 receptor, Nature 581 (7807) (2020) 215–220.
[17] C.B. Jackson, et al., Mechanisms of SARS-CoV-2 entry into cells, Nat. Rev. Mol. Cell Biol. 23 (1) (2022) 3–20.
[18] D. Wrapp, et al., Cryo-EM structure of the 2019-nCoV spike in the prefusion conformation, Science 367 (6483) (2020) 1260–1263.
[19] J. Shang, et al., Structural basis of receptor recognition by SARS-CoV-2, Nature 581 (7807) (2020) 221–224.
[20] S. Xia, et al., The role of furin cleavage site in SARS-CoV-2 spike protein-mediated membrane fusion in the presence or absence of trypsin, Signal Transduct. Targeted Ther. 5 (1) (2020) 1–3.
[21] M.-M. Zhao, et al., Cathepsin L plays a key role in SARS-CoV-2 infection in humans and humanized mice and is a promising target for new drug development, Signal Transduct. Targeted Ther. 6 (1) (2021) 1–12.
[22] M. Hoffmann, et al., SARS-CoV-2 cell entry depends on ACE2 and TMPRSS2 and is blocked by a clinically proven protease inhibitor, Cell 181 (2) (2020) 271–280, e8.
[23] D. Bestle, et al., TMPRSS2 and furin are both essential for proteolytic activation of SARS-CoV-2 in human airway cells, Life science alliance 3 (9) (2020).
[24] H. Zhao, et al., A novel peptide with potent and broad-spectrum antiviral activities against multiple respiratory viruses. Sci Rep 6 (2016) 22008.
[25] N. Zhou, et al., Glycopeptide antibiotics potently inhibit cathepsin l in the late endosome/lysosome and block the entry of ebola virus, middle east respiratory syndrome coronavirus (MERS-CoV), and severe acute respiratory syndrome coronavirus (SARS-CoV), J. Biol. Chem. 291 (17) (2016) 9218–9232.
[26] H. Zhao, et al., Cross-linking peptide and repurposed drugs inhibit both entry pathways of SARS-CoV-2, Nat. Commun. 12 (1) (2021) 1–9.
[27] H. Zhao, et al., A Broad-Spectrum Virus-And Host-Targeting Antiviral Peptide against SARS-CoV-2 and Other Respiratory Viruses, 2020.
[28] S.B. Rathod, et al., Peptide modelling and screening against human ACE2 and spike glycoprotein RBD of SARS-CoV-2, silico pharmacology 8 (1) (2020) 1–9.
[29] R. Bhattacharya, et al., A natural food preservative peptide nisin can interact with the SARS-CoV-2 spike protein receptor human ACE2, Virology 552 (2021) 107–111.
[30] M.S. Baig, et al., Identification of a potential peptide inhibitor of SARS-CoV-2 targeting its entry into the host cells, Drugs R 20 (3) (2020) 161–169.
[31] M. Shah, S.U. Moon, H.G. Woo, Pharmacophore-based Peptide Biologics Neutralize SARS-CoV-2 S1 and Deter S1-ACE2 Interaction in Vitro, 2020 bioRxiv.
[32] Y. Han, P. Král, Computational design of ACE2-based peptide inhibitors of SARS-CoV-2, ACS Nano 14 (4) (2020) 5143–5147.
[33] S. Moradi, et al., Atomistic details on the mechanism of organophosphates resistance in insects: insights from homology modeling, docking and molecular dynamic simulation, J. Mol. Liq. 276 (2019) 59–66.
[34] M. Shahlaei, et al., Cholesterol-lowering drugs the simvastatin and atorvastatin change the protease activity of pepsin: an experimental and computational study, Int. J. Biol. Macromol. 167 (2021) 1414–1423.
[35] R.A. Laskowski, M.B. Swindells, LigPlot+: Multiple Ligand–Protein Interaction Diagrams for Drug Discovery, ACS Publications, 2011.
[36] D. Kozakov, et al., The ClusPro web server for protein–protein docking, Nat. Protoc. 12 (2) (2017) 255–278.
[37] K.A. Porter, et al., ClusPro PeptiDock: efficient global docking of peptide recognition motifs using FFT, Bioinformatics 33 (20) (2017) 3299–3301.
[38] M.J. Abraham, et al., GROMACS: high performance molecular simulations through multi-level parallelism from laptops to supercomputers, Software 1 (2015) 19–25.
[39] N. Schmid, et al., Definition and testing of the GROMOS force-field versions 54A7 and 54B7, Eur. Biophys. J. 40 (7) (2011) 843–856.
[40] U. Stocker, W.F. van Gunsteren, Molecular dynamics simulation of hen egg white lysozyme: a test of the GROMOS96 force field against nuclear magnetic resonance data, Proteins: Structure, Function, and Bioinformatics 40 (1) (2000) 145–153.
[41] B. Hess, et al., LINCS: a linear constraint solver for molecular simulations, J. Comput. Chem. 18 (12) (1997) 1463–1472.
[42] T. Darden, D. York, L. Pedersen, Particle mesh Ewald: an N· log (N) method for Ewald sums in large systems, J. Chem. Phys. 98 (12) (1993) 10089–10092.
[43] R. Kumari, et al., g_mmpbsa A GROMACS tool for high-throughput MM-PBSA calculations, J. Chem. Inf. Model. 54 (7) (2014) 1951–1962.
[44] M.A. Hallen, et al., Osprey 3.0: open-source protein redesign for you, with powerful new features, J. Comput. Chem. 39 (30) (2018) 2494–2507.
[45] S. Gupta, et al., In silico approach for predicting toxicity of peptides and proteins, PLoS One 8 (9) (2013) e73957.
[46] I. Dimitrov, et al., AllerTOP v. 2—a server for in silico prediction of allergens, J. Mol. Model. 20 (6) (2014) 1–6.
[47] R. Yan, et al., Structural basis for the recognition of SARS-CoV-2 by full-length human ACE2, Science 367 (6485) (2020) 1444–1448.
[48] C.G. Benítez-Cardoza, J.L. Vique-Sánchez, Potential inhibitors of the interaction between ACE2 and SARS-CoV-2 (RBD), to develop a drug, Life Sci. 256 (2020) 117970.
[49] A. Hussain, et al., Targeting SARS-CoV2 Spike Protein Receptor Binding Domain by Therapeutic Antibodies, Biomedicine & Pharmacotherapy, 2020, p. 110559.
[50] A.C. Pushkaran, et al., A phytochemical-based medication search for the SARS-CoV-2 infection by molecular docking models towards spike glycoproteins and main proteases, RSC Adv. 11 (20) (2021) 12003–12014.
[51] M. Prajapat, et al., Virtual screening and molecular dynamics study of approved drugs as inhibitors of spike protein S1 domain and ACE2 interaction in SARS-CoV-2, J. Mol. Graph. Model. 101 (2020) 107716.
[52] W. Dongyuan, L. Zigang, L. Yihui, An overview of the safety, clinical application and antiviral research of the COVID-19 therapeutics, Journal of infection and public health 13 (10) (2020) 1405–1414.
[53] D.P. Han, A. Penn-Nicholson, M.W. Cho, Identification of critical determinants on ACE2 for SARS-CoV entry and development of a potent entry inhibitor, Virology 350 (1) (2006) 15–25.
[54] P. Pei, et al., Computational design of ultrashort peptide inhibitors of the receptor-binding domain of the SARS-CoV-2 S protein, Briefings Bioinf. 22 (6) (2021) bbab243.
[55] A. Kuznetsov, et al., ACE2 peptide fragment interaction with different S1 protein sites, Int. J. Pept. Res. Therapeut. 28 (1) (2022) 1–7.
[56] N. Fernandez-Fuentes, R. Molina, B. Oliva, A collection of designed peptides to target SARS-CoV-2 spike RBD—ACE2 interaction, Int. J. Mol. Sci. 22 (21) (2021) 11627.
[57] J. Chen, et al., Inhibition of SARS-CoV-2 pseudovirus invasion by ACE2 protecting and Spike neutralizing peptides: an alternative approach to COVID19 prevention and therapy, Int. J. Biol. Sci. 17 (11) (2021) 2957.
[58] Y. Badhe, R. Gupta, B. Rai, In silico design of peptides with binding to the receptor binding domain (RBD) of the SARS-CoV-2 and their utility in bio-sensor development for SARS-CoV-2 detection, RSC Adv. 11 (7) (2021) 3816–3826.
[59] S.K. Panda, et al., ACE-2-derived biomimetic peptides for the inhibition of spike protein of SARS-CoV-2, J. Proteome Res. 20 (2) (2021) 1296–1303.
[60] A.R. Choudhury, et al., Computational Design of Stapled Peptide Inhibitor against SARS-CoV-2 Receptor Binding Domain, 2021.
[61] A. Basit, T. Ali, S.U. Rehman, Truncated human angiotensin converting enzyme 2; a potential inhibitor of SARS-CoV-2 spike glycoprotein and potent COVID-19 therapeutic agent, J. Biomol. Struct. Dyn. 39 (10) (2021) 3605–3614.
[62] S. Kianipour, et al., A molecular dynamics study on using of naturally occurring polymers for structural stabilization of erythropoietin at high temperature, J. Biomol. Struct. Dyn. (2021) 1–11.
[63] K.S. Ebrahimi, et al., In silico investigation on the inhibitory effect of fungal secondary metabolites on RNA dependent RNA polymerase of SARS-CoV-II: a

docking and molecular dynamic simulation study, Comput. Biol. Med. 135 (2021) 104613.
[64] M.I. Barton, et al., Effects of common mutations in the SARS-CoV-2 Spike RBD and its ligand, the human ACE2 receptor on binding affinity and kinetics, Elife 10 (2021) e70658.
[65] S.A. Andújar, et al., Structure, interface stability and hot-spots identification for RBD (SARS-CoV-2): hACE2 complex formation, Mol. Simulat. 47 (17) (2021) 1443–1454.